Supplemental Material for

On the need for physical constraints in deep leaning rainfall-runoff projections under climate change

Sungwook Wi[1], **Scott Steinschneider**[1]

[1]Department of Biological and Environmental Engineering, Cornell University, Ithaca, NY, USA

Summary

This supplementary material file contains six figures in support of the analysis and conclusions presented in the main article.

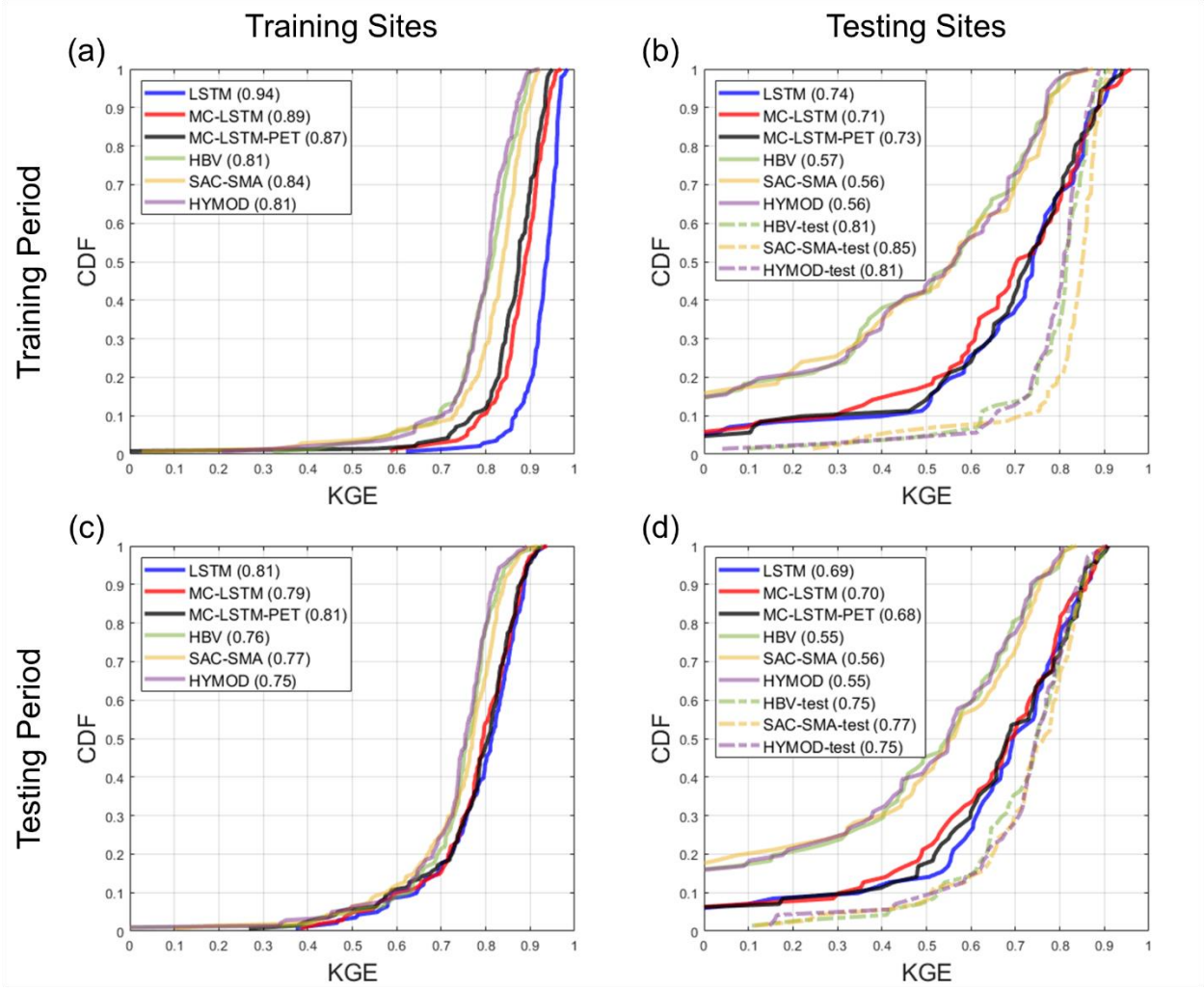

Figure S1. The distribution of Kling-Gupta efficiency (KGE) for streamflow estimates across sites from each model at the (a) 141 training sites and (b) 71 testing sites for the training period. Similar results for the testing period are shown in panels (c) and (d), respectively. For the process models fit to the testing sites (denoted "-test"), no performance results are available at the training sites. All models are trained using Hamon PET.

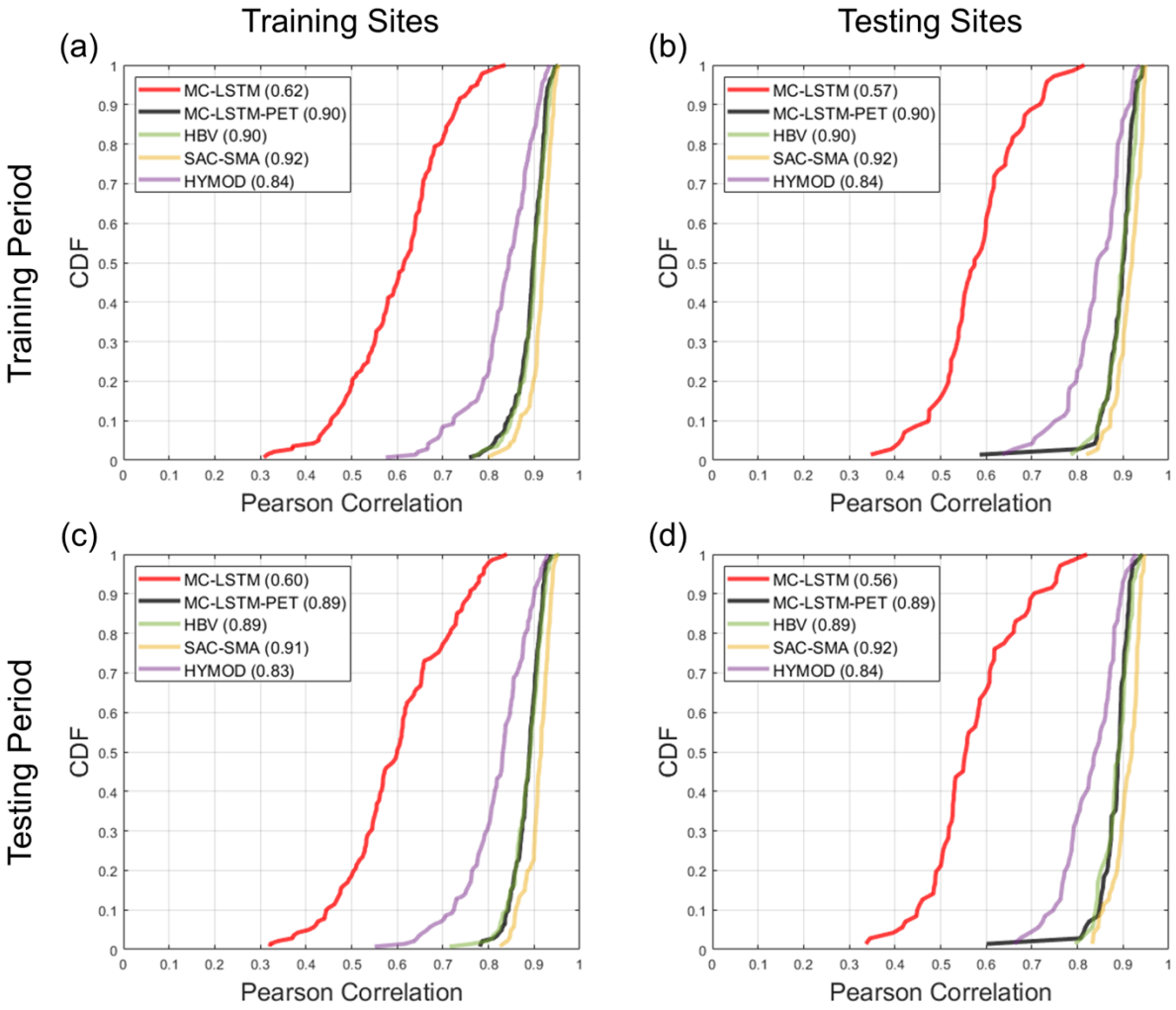

Figure S2. The correlation between model estimated and observed AET from each model at the (a) 141 training sites and (b) 71 testing sites for the training period. Similar results for the testing period are shown in panels (c) and (d), respectively. The LSTM is not included in this comparison. All models are trained using Priestley-Taylor PET.

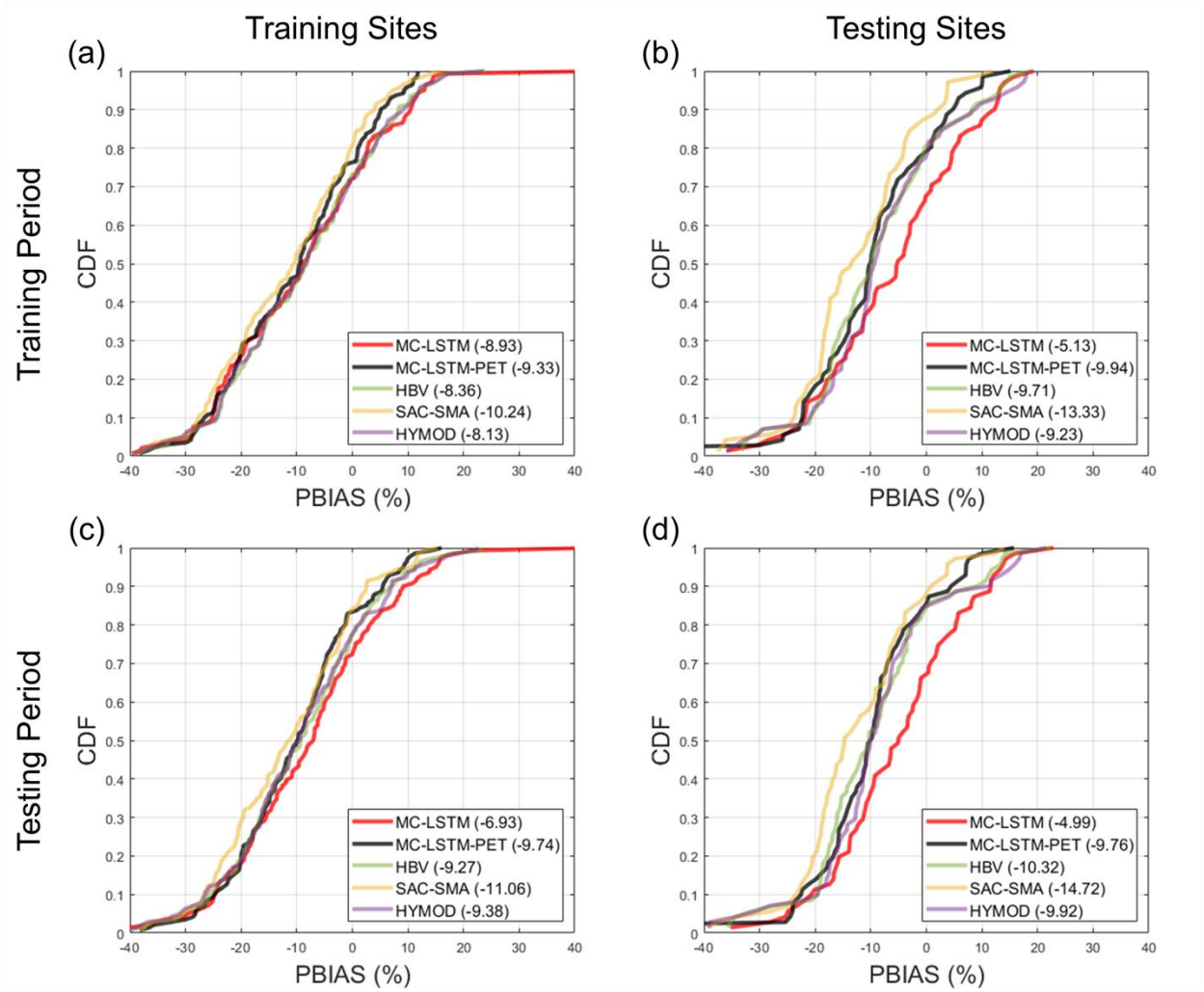

Figure S3. The PBIAS between model estimated and observed AET from each model at the (a) 141 training sites and (b) 71 testing sites for the training period. Similar results for the testing period are shown in panels (c) and (d), respectively. The LSTM is not included in this comparison. All models are trained using Priestley-Taylor PET.

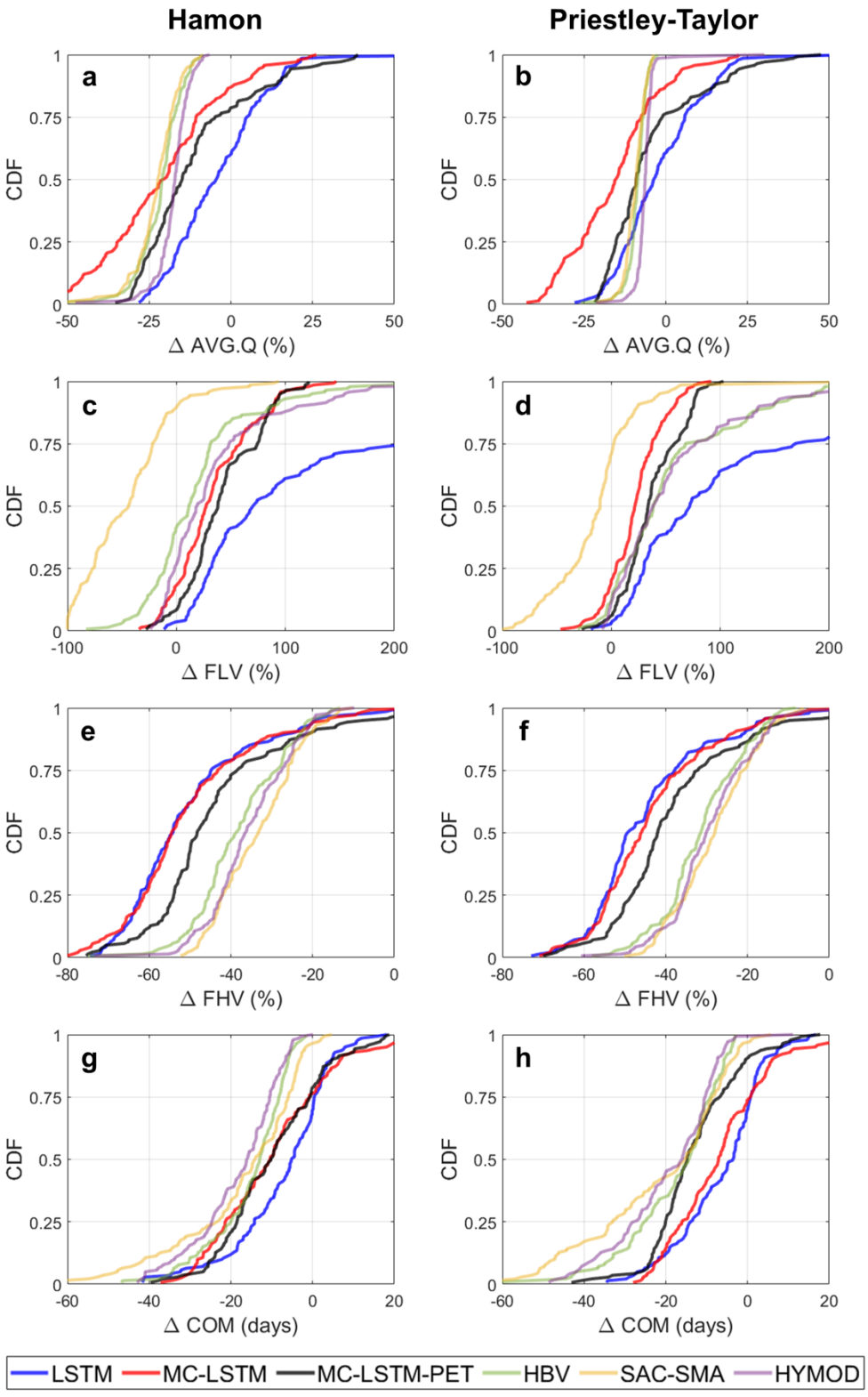

Figure S4. The distribution of change in (a,b) AVG.Q, (c,d) FLV, (e,f) FHV, and (g,h) COM across the 141 training sites and all models under a scenario of 4°C warming using (a,c,e,g) Hamon PET and (b,d,f,h) Priestley-Taylor PET. For the DL models, changes were made to both the dynamic and static inputs.

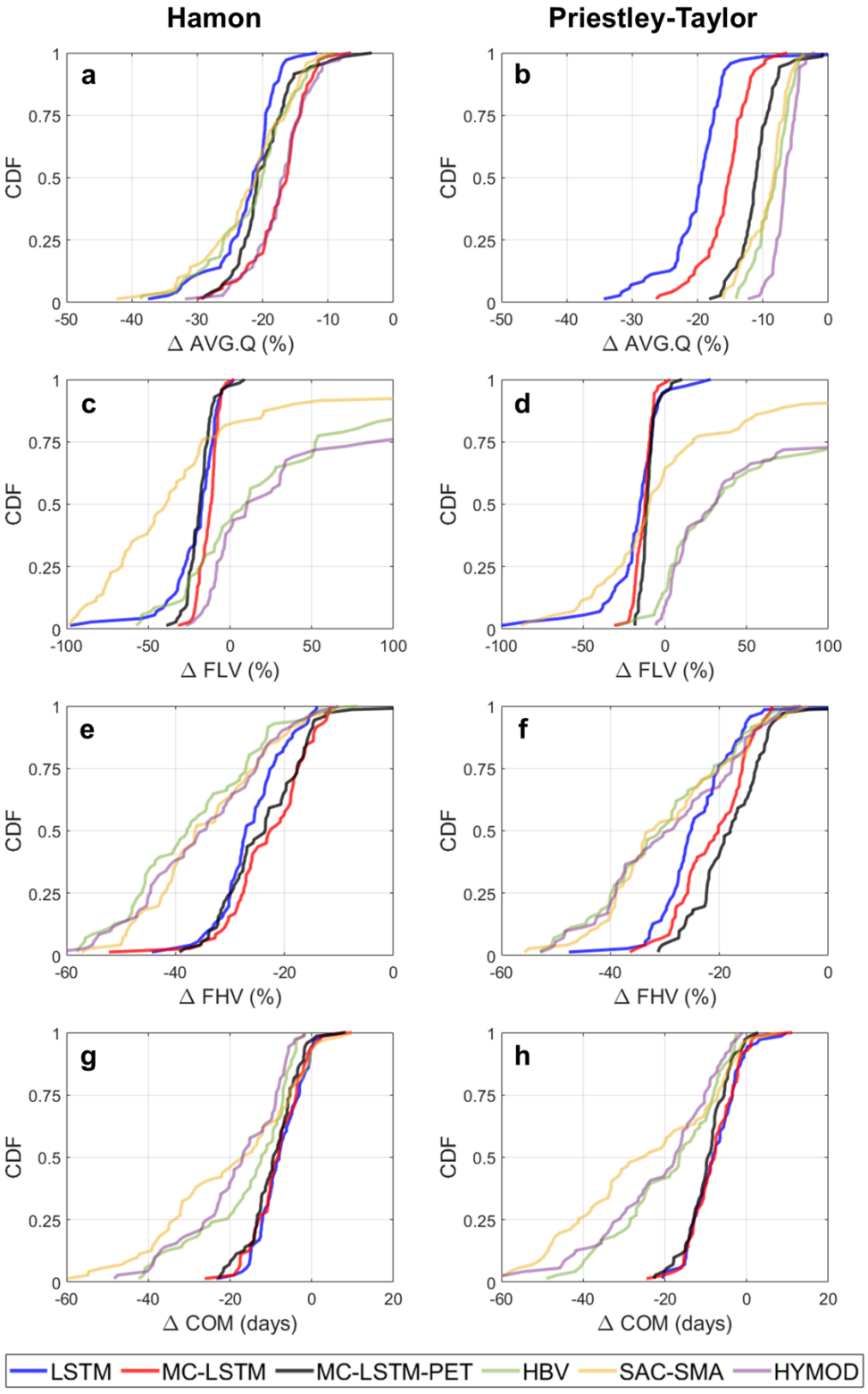

Figure S5. The distribution of change in (a,b) AVG.Q, (c,d) FLV, (e,f) FHV, and (g,h) COM across the 71 testing sites and all models under a scenario of 4°C warming using (a,c,e,g) Hamon PET and (b,d,f,h) Priestley-Taylor PET. For the DL models, changes were only made to the dynamic inputs (i.e., no changes to static inputs).

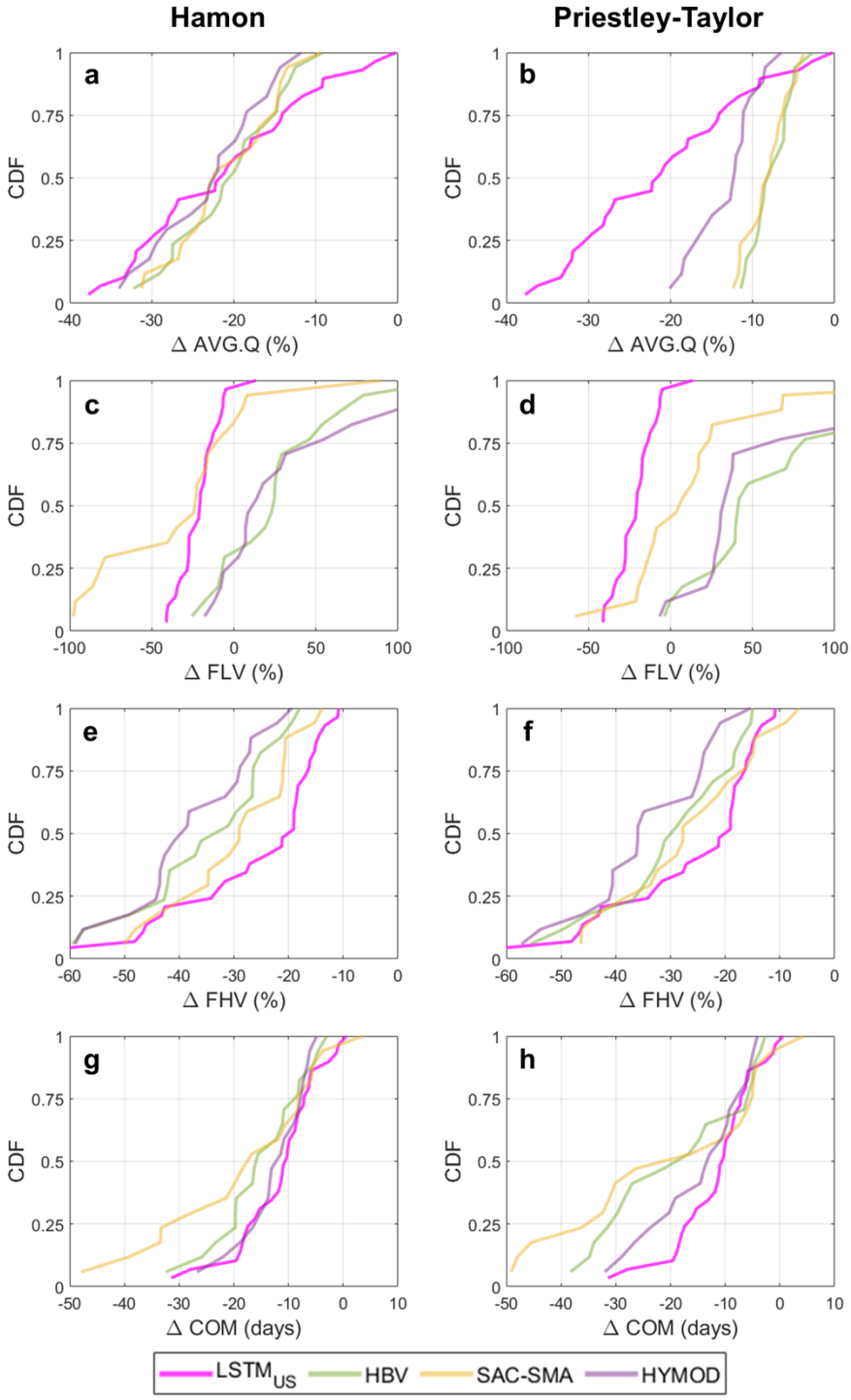

Figure S6. The distribution of change in (a,b) AVG.Q, (c,d) FLV, (e,f) FHV, and (g,h) COM across 29 CAMELS sites within the Great Lakes basin under the National LSTM, as well as for 17 of those 29 sites from the Great Lakes process models, under a scenario of 4°C warming. For the process models only, results differ when using (a,c,e,f) Hamon PET and (b,d,f,h) Priestley-Taylor PET. For the National LSTM, changes were made to both the dynamic and static inputs.